Markovian and non-Markovian dynamics induced by a generic environment

M. Carrera,[1] T. Gorin,[2] and C. Pineda[3,*]

[1]*Instituto de Física, Benemérita Universidad Autónoma de Puebla, Apartado Postal J-48, Puebla 72570, Mexico*
[2]*Departamento de Física, Universidad de Guadalajara, Blvd. Marcelino García Barragan y Calzada Olímpica, Guadalajara C.P. 44840, Jalísco, Mexico*
[3]*Instituto de Física, Universidad Nacional Autónoma de México, México D.F. 01000, Mexico*

(Received 27 June 2019; published 21 October 2019)

We study the open dynamics of a quantum two-level system coupled to an environment modeled by random matrices. Using the quantum channel formalism, we investigate different quantum Markovianity measures and criteria. A thorough analysis of the whole parameter space reveals a wide range of different regimes, ranging from strongly non-Markovian to Markovian dynamics. In contrast to analytical models, all non-Markovianity measures and criteria have to be applied to data with fluctuations and statistical uncertainties. We discuss the practical usefulness of the different approaches.

DOI: 10.1103/PhysRevA.100.042322

I. INTRODUCTION

Open quantum systems have been of interest for a long time [1]. The interest stems from the natural separation of a quantum system into a central system of interest, and an uninteresting or uncontrollable part, usually denoted by *environment*. In 1967, Lindblad [2] and Gorini, Kossakowski, and Sudarshan [3] arrived at the so-called Lindblad master equation to describe the evolution of a central system weakly interacting with a memoryless environment. This equation has been of paramount importance in the field as one can both analytically solve several instances of the equation [4] and describe accurately a wide range of experimental situations [5]. The dynamics produced by such an equation is called *quantum Markovian dynamics*. Recently there has been an effort to classify and understand systematically open quantum systems which lie outside this description.

Definitions and measures for quantum non-Markovianity (NM) have received considerable interest in the last 10 years or so [6,7]. They are meant to characterize quantum processes (*viz.*, the dynamics of open quantum systems) which cannot be described by a master equation with constant Lindblad operators. For such systems, one might wish to establish an order relation of increasing non-Markovianity in the sense that it is increasingly difficult to describe the quantum process by some effective evolution equation within the system's state space alone. A second quite different idea is that NM is a feature which might be taken advantage of in order to perform certain tasks. Both are valid points of view, but it is not clear to what extend some of the popular definitions and measures of NM provide relevant information with respect to these questions. Several reviews of the field can be found in Refs. [8–11].

Non-Markovianity has been studied extensively for quantum processes with an analytical solution, implying no fluctuations or uncertainties; however, applications to more realistic processes are relatively rare [12,13].

In the present paper, we study a quantum channel derived from the coupling of a two-level system to a "generic" quantum environment. We use random matrix theory (RMT) to describe that environment. Choosing the Hamiltonian in the environment from the Gaussian unitary ensemble, we find a variety of different behaviors in the relevant parameter space, ranging from Markovian (Lindblad dynamics) to strongly NM behavior. This model is ideal to discuss the questions raised above. Since the model has no known analytical solution, all criteria and measures must be calculated numerically, with unavoidable statistical errors, which resembles an experimental situation in which finite statistics come into play.

In Sec. II we present the model and find the structure of the quantum channel describing the dynamics of the system. In Sec. III we introduce the NM measures, which we will use in Sec. IV for analysis. In Sec. IV we compare and interpret the different measures for the whole available region in the parameter space. We finish with some closing remarks in Sec. V.

II. MODEL

In this section we introduce a random matrix model, which is suitable to describe open quantum systems in several contexts. Wigner was probably the first to use random matrices to describe physical systems, specifically compound nuclei [14], which may be considered prime examples of complex multiparticle systems. Subsequently, RMT has been found to be applicable to quantum chaotic [15] and disordered systems [16], both being typically treated in a (effective) single particle picture. In the context of quantum information, the usage of this techniques, has allowed to calculate, e.g., fidelities for gate operations and has produced proposals to increase the robustness of quantum computers under generic errors [17]. In a similar context, random matrices were proposed both as a model for environments which are describable within an effectively finite dimensional Hilbert space, e.g., spin networks [18,19], or which consist of only a few relevant degrees of freedoms [20]. In both cases, the equilibration of the dynamics which usually goes along with the thermodynamic limit is taken care of by quantum chaos or disorder [21–25].

*carlospgmat03@gmail.com

For the dynamics of the composite system, one typically starts with the environment in an equilibrium state, and the central system being prepared independently, in an arbitrary known initial state. The quantity of interest is then the reduced state of the central system in the presence of the coupling between system and environment. There are several possible choices for the equilibrium state of the environment: First, we have a microcanonical mixture of energy eigenstates, lying in a narrow energy interval [20]. Second, there is a thermal mixture of energy eigenstates. Eventually, that case can be obtained by averaging the result under the first with the given thermal probability distribution [26]. Third, we have a uniform mixture in a finite Hilbert space that we assume here for convenience, as it avoids dragging along another parameter. From a physical point of view, that choice corresponds to taking a high temperature limit.

The particular model to be used here has been introduced in Ref. [27], which focused on the derivation of an analytical description in the linear response regime. We find it suitable for the purpose of the present work, since it is a generic model, which, nonetheless shows a broad range of different behaviors with respect to quantum NM. In this section, we describe the Hamiltonian of our system and the quantum channel formalism used for a complete description of its dynamics.

A. The Hamiltonian

We consider a two-level system (qubit) coupled to an environment. The Hilbert space of the qubit will be labeled by the subindex $_c$ and that of the environment by the subindex $_e$. We assume that the dynamics in the whole Hilbert space is unitary, with the evolution governed by the Hamiltonian

$$H_\lambda = \frac{\Delta}{2}\sigma_z \otimes \mathbb{1}_e + \mathbb{1}_c \otimes H_e + \lambda\, v_c \otimes V_e. \tag{1}$$

All subindices of operators in the right-hand side indicate the subspace in which they act, except for σ_z, which is a Pauli matrix acting on the qubit. Δ is the level splitting in the qubit, and the parameter λ controls the strength of the coupling between the central system and the environment. The first two terms in Eq. (1) represent the free evolution of both central system and environment, while the third term provides the coupling which is assumed to be separable. The Hamiltonian of the environment H_e shall be chosen from the Gaussian unitary ensemble to provide generality to the results discussed here [28]. We measure time in units of the Heisenberg time of H_e and energy in units of the means level spacing in the center of the spectrum of H_e; in such units, $\hbar = 1$. The density matrix of the central system for a time t is given by

$$\varrho_c(t) = \mathrm{tr}_e\big[\big\langle e^{-iH_\lambda t}\, \varrho_c \otimes \varrho_e\, e^{iH_\lambda t}\big\rangle\big], \tag{2}$$

where we have chosen a product state as the initial state of central system and environment. Just as H_e, V_e is also chosen from the Gaussian unitary ensemble, and the angular brackets denote an ensemble average over both random matrices. The magnitude of the matrix elements $[V_e]_{ij}$ is chosen such that $\langle [V_e]_{ij}[V_e]_{kl}\rangle = \delta_{il}\delta_{jk}$.

The most general form of v_c has a parallel and perpendicular component, with respect to the internal Hamiltonian σ_z. If there is only a parallel component ($v_c \propto \sigma_z$) the qubit dynamics becomes dephasing. The channel acting on the qubit can be obtained in terms of the fidelity amplitude for the Hamiltonians $H_e \pm \lambda V_e$. This is already a very rich case; however, it has been considered before [21,29]. The other limiting case is when the coupling is perpendicular to the internal Hamiltonian, which is the case we are studying here; see also Ref. [27]. Thus we simply set, without losing any generality,

$$v_c = \sigma_x, \tag{3}$$

where σ_x is one of the three Pauli matrices. In the environment, we choose the initial state to be the maximally mixed state, $\varrho_e \propto \mathbb{1}$, the high temperature limit of a Gibbs state in a finite dimensional Hilbert space. That choice eases the forthcoming mathematical calculations, but a finite temperature Gibbs state could be considered equally well.

B. Quantum channel formalism

We describe the reduced dynamics of the qubit with the quantum channel formalism, which means that the evolution of the system state is described in terms of a linear time dependent map Λ_t acting on the space of density matrices $\mathcal{S}(\mathbb{C}^2)$ of the central system. The map Λ_t takes an arbitrary initial state, and returns the state evolved according to Eq. (2) for a time t,

$$\Lambda_t \;:\; \varrho_c \to \varrho_c(t) = \Lambda_t[\varrho_c]. \tag{4}$$

Since the image of this map is a density matrix, Λ_t has two properties: it (1) preserves the trace of the argument and (2) is completely positive. Maps with these characteristics will be referred to as *quantum channels*. We will also be interested in more general linear operators that preserve the trace but, even though they map Hermitian operators to Hermitian operators, are not necessarily completely positive. In fact, we shall consider maps that are generally nonpositive. We will call such maps *quantum maps*. In this language, a quantum channel is a quantum map, but not necessarily the other way around.

A quantum map K, and any linear map, is determined by its action on a basis; consider the computational basis $\{|a\rangle\langle b|\}_{a,b\in\{0,1\}}$ and arrange the resulting elements in the matrix

$$C_K = \begin{pmatrix} K[|0\rangle\langle 0|] & K[|0\rangle\langle 1|] \\ K[|1\rangle\langle 0|] & K[|1\rangle\langle 1|] \end{pmatrix}. \tag{5}$$

This is the so-called Choi-matrix representation [30,31]. Since K maps Hermitian matrices to Hermitian matrices, C_K must also be Hermitian.

It can be seen that the Choi matrix can be obtained by applying the extended map id $\otimes K$ to a Bell state in the Hilbert space of two qubits:

$$C_K = 2\,(\mathrm{id} \otimes K)\,[|\mathrm{Bell}\rangle\langle\mathrm{Bell}|], \tag{6}$$

where $|\mathrm{Bell}\rangle = (|00\rangle + |11\rangle)/\sqrt{2}$. Thus, if K is a quantum channel, $1/2\,C_K$ is a two-qubit density matrix, which in turn implies that $C_K \geqslant 0$, i.e., all of its eigenvalues must be positive or equal to zero.

We will now outline the procedure to construct the Choi matrix, $C_t \equiv C_{\Lambda_t}$, describing the dynamics defined in Eq. (2). The procedure will rely on two properties of our particular

channel. First, it is unital, which means that the identity is mapped onto the identity. Second, the evolution of a diagonal operator remains diagonal, i.e., if ϱ_c is diagonal, so is $\varrho_c(t)$ in Eq. (4). The proof of both properties is found in Appendix A. This implies that the Choi matrix is of the form

$$C_t \equiv C_{\Lambda_t} = \begin{pmatrix} r & 0 & 0 & z_1^* \\ 0 & 1-r & z_2 & 0 \\ 0 & z_2^* & 1-r & 0 \\ z_1 & 0 & 0 & r \end{pmatrix}, \tag{7}$$

where time-dependent functions $r \equiv r(t)$, $z_1 \equiv z_1(t)$, and $z_2 \equiv z_2(t)$ with $r(0) = z_1(0) = 1$, and $z_2(0) = 0$. The particular shape of C_t means for the representation in the Bloch sphere that the dynamics along the z axis is decoupled from the dynamics in the xy plane.

Let $\varrho_c^{x,y,z}$ be the density matrices associated with the positive eigenvalues of the corresponding Pauli matrices. From the second property and trace conservation, we find that

$$\Lambda_t[\varrho_c^z] = \begin{pmatrix} r & 0 \\ 0 & 1-r \end{pmatrix}, \tag{8}$$

and from the first property, plus linearity of quantum maps, we get

$$\Lambda_t[\varrho_c^x] = \frac{1}{2}\begin{pmatrix} 1 & z_x^* \\ z_x & 1 \end{pmatrix}, \quad \Lambda_t[\varrho_c^y] = \frac{1}{2}\begin{pmatrix} 1 & z_y^* \\ z_y & 1 \end{pmatrix} \tag{9}$$

with $z_{1,2} = (z_x \mp i z_y)/2$. In conclusion, we can reconstruct the Choi matrix C_t of the quantum process of interest by calculating numerically the time evolution of the eigenstates $\varrho_c^{x,y,z}$ of the Pauli matrices.

III. NON-MARKOVIANITY MEASURES

We consider NM as a property of a quantum process Λ_t, which is a one-parameter family of quantum channels with $t \in \mathbb{R}_0^+$ and $\Lambda_0 = \mathrm{id}$. The NM criteria and measures used here are based on two different concepts, (1) divisibility and (2) contractivity. Both of them require knowledge of the intermediate quantum map

$$\Lambda_{t+\varepsilon,t} = \Lambda_{t+\varepsilon} \circ \Lambda_t^{-1} \quad : \quad \varrho \to \Lambda_{t+\varepsilon}\big[\Lambda_t^{-1}[\varrho]\big]. \tag{10}$$

In Appendix B 1, we calculate the Choi representation of this intermediate quantum map with the following result:

$$C_{t+\varepsilon,t} = \begin{pmatrix} q & 0 & 0 & Z_1^* \\ 0 & 1-q & Z_2 & 0 \\ 0 & Z_2^* & 1-q & 0 \\ Z_1 & 0 & 0 & q \end{pmatrix}, \tag{11}$$

with $D = |z_1|^2 - |z_2|^2$, $Z_1 = (z_1' z_1^* - z_2' z_2^*)/D$, $Z_2 = (z_2' z_1 - z_1' z_2)/D$, and $q = (r + r' - 1)/(2r - 1)$. The parameters r', z_1', and z_2' are the same as r, z_1, and z_2 but calculated at a time $t + \varepsilon$. When $D = 0$ or $2r - 1 = 0$, Λ_t is not invertible, and therefore $\Lambda_{t+\varepsilon,t}$ may not exist.

A. Divisibility

A quantum process Λ_t is divisible if and only if for any $t, \varepsilon > 0$ it holds that $\Lambda_{t+\varepsilon}$ can be written as the composition $\Lambda_{t+\varepsilon} = \Lambda_x \circ \Lambda_t$, with Λ_x being a valid quantum channel. Here, Λ_x can be identified with the intermediate quantum map $\Lambda_{t+\varepsilon,t}$ given in Eq. (10). Hence the divisibility of a quantum process is equivalent to all intermediate quantum maps being valid quantum channels. Formally speaking, the quantum process Λ_t is divisible if and only if

(a) Λ_t is invertible for almost all $t \in \mathbb{R}_0^+$, and

(b) $\forall t, \varepsilon > 0 : \Lambda_{t+\varepsilon,t} = \Lambda_{t+\varepsilon} \circ \Lambda_t^{-1}$ is a valid quantum channel if it exists.

In condition (a), we allow Λ_t to be noninvertible at a finite (countable) number of points in time. In condition (b), we check the complete positivity of the intermediate map only for those t, where Λ_t is invertible.

1. RHP Markovianity

One of the definitions of NM is given in terms of the divisibility of the quantum process under consideration. Following Rivas *et al.* [7], we call a quantum process Λ_t, RHP Markovian if and only if the two conditions above are fulfilled.

To check for the complete positivity of the intermediate quantum map, Rivas *et al.* consider the trace norm of the associated Choi matrix defined as $\|C_{t+\varepsilon,t}\|_1 = \sum_j |\lambda_j|$, where λ_j are the eigenvalues of $C_{t+\varepsilon,t}$. Since the sum of the eigenvalues always is equal to the dimension of the Hilbert space of the physical system, due to trace preservation, any negative eigenvalue will necessarily lead to $\|C_{t+\varepsilon,t}\|_1$ being larger than two. In addition, since the composition of two quantum channels is again a quantum channel, it is sufficient to check complete positivity for infinitesimal ε only. Hence, Rivas *et al.* define the function

$$g(t) = \lim_{\varepsilon \to 0} \frac{1}{2\varepsilon} \left(\|C_{t+\varepsilon,t}\|_1 - 2\right), \tag{12}$$

which is zero if the intermediate map is completely positive, and greater than zero otherwise. Moreover, to define a measure of the degree of non-Markovianity of the process, the authors integrate this function over time. We shall label this quantity as

$$\mathcal{N}_{\mathrm{RHP}}(t) = \int_0^t d\tau \; g(\tau). \tag{13}$$

Notice that $\mathcal{N}_{\mathrm{RHP}}(t) = 0$ if and only if the process is divisible for all times up to t.

2. Application to our model

In order to check the RHP-Markovianity (divisibility) of Λ_t as defined in Sec. II, we use the Choi representation, Eq. (11) of the intermediate quantum map $\Lambda_{t+\varepsilon,t}$. The eigenvalues of $C_{t+\varepsilon,t}$ are

$$\lambda_{1,2} = q \pm |Z_1|, \quad \lambda_{3,4} = (1-q) \pm |Z_2|. \tag{14}$$

Hence, the eigenvalues are non-negative if and only if (1) $|Z_1| \leqslant q$ and (2) $|Z_2| \leqslant 1 - q$.

Since we can limit to infinitesimal ε, we expand the different functions in Eq. (11) around t and obtain, to first order,

$$Z_1 = 1 + \frac{\varepsilon}{D}(\dot{z}_1 z_1^* - \dot{z}_2 z_2^*), \tag{15}$$

$$Z_2 = \frac{\varepsilon}{D}(\dot{z}_2 z_1 - \dot{z}_1 z_2),$$

$$q = 1 + \frac{\varepsilon \dot{r}}{2r - 1}, \tag{16}$$

where we have used the fact that $r' = r + \varepsilon\,\dot{r}$, $z_1' = z_1 + \varepsilon\,\dot{z}_1$, and $z_2' = z_2 + \varepsilon\,\dot{z}_2$.

The two conditions can now be written as

$$\begin{aligned} &\text{(i)} && 1 - \varepsilon\,\delta_1 \leqslant 1 - \varepsilon\,\delta_q && \Leftrightarrow && \delta_1 \geqslant \delta_q, \\ &\text{(ii)} && |Z_2| \leqslant 1 - q && \Leftrightarrow && \delta_2 \leqslant \delta_q, \end{aligned} \tag{17}$$

where we introduced

$$\delta_1 = -\frac{1}{D}\,\mathrm{Re}[\dot{z}_1 z_1^* - \dot{z}_2 z_2^*], \tag{18}$$

$$\delta_q = \frac{-\dot{r}}{2r-1} \geqslant 0, \tag{19}$$

and

$$\delta_2 = \frac{|\dot{z}_2 z_1 - \dot{z}_1 z_2|}{|D|}. \tag{20}$$

Additionally we used the fact that for any complex number c, $|1 + \varepsilon c| = 1 + \varepsilon c + O(\varepsilon^2)$ in the expression for $|Z_1|$. Finally, we combine the two inequalities into

$$\delta_2 \leqslant \delta_q \leqslant \delta_1. \tag{21}$$

We can now relate our inequalities to the criterium of Rivas *et al.* as follows. In our case, the trace norm of the Choi matrix can be written as

$$\begin{aligned} ||C_{t+\varepsilon,t}||_1 &= |q + |Z_1|| + |q - |Z_1|| + |1 - q + |Z_2|| \\ &\quad + |1 - q - |Z_2|| \\ &= 2 - \varepsilon\,(\delta_q + \delta_1 - |\delta_1 - \delta_q| - |\delta_q \\ &\quad + \delta_2| - |\delta_q - \delta_2|). \end{aligned} \tag{22}$$

This yields

$$g(t) = \frac{|\delta_1 - \delta_q| + |\delta_q + \delta_2| + |\delta_q - \delta_2| - \delta_q - \delta_1}{2}. \tag{23}$$

We showed that non-negativity of the eigenvalues is equivalent to the double inequality $\delta_2 \leqslant \delta_q \leqslant \delta_1$. Then we saw that it is also equivalent to $g(t) = 0$. This means that the double inequality holds if and only if $g(t) = 0$.

B. Contractivity

Markovianity of classical stochastic processes implies that probabilities distributions decrease their Kolmogorov distance with time [32]. This is interpreted as a loss of information of the initial conditions. Carrying this idea to a quantum level results in a definition of Markovianity [6]. Let $\varrho_{1,2}(t)$ denote the evolution of two states $\varrho_{1,2}$. We define

$$\sigma(\varrho_1, \varrho_2, t) = \frac{d}{dt} T[\varrho_1(t), \varrho_2(t)], \tag{24}$$

where $T[\varrho_1(t), \varrho_2(t)] = \mathrm{tr}(|\varrho_1(t) - \varrho_2(t)|)/2$ is the trace distance, which is directly related to the probability of distinguish the state $\varrho_1(t)$ from the state $\varrho_2(t)$, i.e., it is their distinguishability [33], and $|A| = \sqrt{AA^\dagger}$. In other words, σ is the derivative of the distance between the evolved states. We say that a process is contractive if for all $\varrho_{1,2}$ and all $t \geqslant 0$, we have that $\sigma(\varrho_1, \varrho_2, t) \leqslant 0$. A process is said to be non-Markovian if it is not contractive. Breuer *et al.* then define the following quantity as a measure for the degree of non-Markovianity:

$$\mathcal{N}_{\mathrm{BLP}}(t) = \max_{\varrho_1,\varrho_2} \int_{0\leqslant\tau\leqslant t,\sigma>0} d\tau\ \ \sigma(\varrho_1, \varrho_2, \tau). \tag{25}$$

The calculation of this measure is greatly simplified when the process acts on a qubit. To perform this maximization, one should consider only pure, orthogonal initial states [34]. Indeed, we found that $T[\varrho_1(t), \varrho_2(t)]$ depends only on the vector difference between the representations of initial states in the Bloch ball (see Appendix B 2). Moreover, the distance between the two points representing the initial states enters as a homogeneous scale factor. It therefore possible, restricting the maximum search to such cases, where ϱ_1 is a pure state, and ϱ_2 the uniform mixture. If the pure state ϱ_1 is parametrized in spherical coordinates by the angles θ and ϕ, we obtain [cf. Eq. (B11)]

$$\begin{aligned} \sigma(\varrho_1, \mathbb{1}/2, t) &= \frac{1}{2}\frac{d}{dt}\,||\sin\theta(\cos\phi\sigma_x + \sin\phi\sigma_y) + \cos\theta\sigma_z|| \\ &= \frac{1}{2}\frac{d}{dt}\sqrt{(2r-1)^2\cos^2\theta + M(\phi)\sin^2\theta}, \end{aligned} \tag{26}$$

with $M(\phi) = |z_1 + z_2\,e^{-2i\phi}|^2$.

In what follows, we derive a criteria for NM based on the contractivity, which can be compared to the criteria Eq. (21) obtained in Sec. III A, based on divisibility. Since θ may be chosen freely in Eq. (26), a given process is Markovian in the sense of Breuer *et al.*, if and only if both functions, $(2r-1)^2$ and $M(\phi)$ are nonncreasing at all times. In other words if

$$\frac{d}{dt}(2r-1)^2 \leqslant 0, \tag{27}$$

$$\frac{d}{dt}M(\phi) \leqslant 0 \tag{28}$$

for all times, condition (27) becomes $-\dot{r}(2r-1) = \delta_q(2r-1)^2 \geqslant 0$, which in turn is equivalent to $\delta_q \geqslant 0$ (at least as long as $2r - 1 \neq 0$, i.e., away from the points where Λ_t is not invertible). To consider condition (28), we expand $M(\phi)$ as

$$M(\phi) = A + \cos(2\phi)\,B - \sin(2\phi)\,C, \tag{29}$$

where $A = |z_1|^2 + |z_2|^2$, $B = 2\,\mathrm{Re}(z_1 z_2^*)$, and $C = 2\,\mathrm{Im}(z_1 z_2^*)$. Setting $\dot{B} = R\cos\alpha$ and $\dot{C} = R\sin\alpha$, we define R and α via the equations $\dot{B} = R\cos\alpha$ and $\dot{C} = R\sin\alpha$, so one can write

$$\frac{d}{dt}M(\phi) = \dot{A} + \sqrt{\dot{B}^2 + \dot{C}^2}\cos(2\phi + \alpha). \tag{30}$$

From this, it is clear that the largest time derivative of $M(\phi)$ is $\dot{M}_{\max} = \dot{A} + \sqrt{\dot{B}^2 + \dot{C}^2}$. With $Z = z_1 z_2^*$, we find $\dot{B} = \dot{Z} + \dot{Z}^*$ and $\dot{C} = -i\,(\dot{Z} - \dot{Z}^*)$ such that

$$\dot{M}_{\max} = \dot{A} + \sqrt{(\dot{Z} + \dot{Z}^*)^2 - (\dot{Z} - \dot{Z}^*)^2} = \dot{A} + 2|\dot{Z}|. \tag{31}$$

To summarize, for the process to be Markovian (in the sense of contractivity), it is required that both $\delta_q \geqslant 0$ and $\dot{M}_{\max} \leqslant 0$. This is equivalent to

$$\delta_q \geqslant 0, \quad \delta_1^{\mathrm{C}} \geqslant \delta_2^{\mathrm{C}}, \tag{32}$$

where

$$\delta_2^{\mathrm{C}} = |\dot{z}_1 z_2^* + z_1 \dot{z}_2^*|, \quad \delta_1^{\mathrm{C}} = -\mathrm{Re}(\dot{z}_1 z_1^* + \dot{z}_2 z_2^*). \tag{33}$$

This double inequality is the analog of Eq. (21), which has been derived as criterium for Markovianity in the sense of divisibility.

For unital maps like the one considered here, contractivity of the trace distance can be identified with positivity. That means that our quantum process Λ_t is contractive if and only if all intermediate maps are positive. Note that divisibility is defined as all intermediate maps being completely positive. Thus, there may be processes which are contractive but not divisible [35]. Therefore, we may find regions in the parameter space of our system, where the dynamics is contractive (i.e., BLP Markovian) but not divisible (i.e., RHP Markovian). A recent, comprehensive discussion on different criteria for divisible and contractive processes can be found in Ref. [36].

C. Maximal recovery

This quantifier of non-Markovianity can be based on any capacity-like property of the channel. In fact, we use distinguishability, maximized over states, such as in the case of the BLP measure. However, instead of summing up all the small increments, we search for the maximum distinguishability recovery over the whole quantum process [25]:

$$\mathcal{N}_{\mathrm{MDR}}(t) = \max_{\substack{t \geqslant t_1 \geqslant t_2 \geqslant 0 \\ \varrho_1,\, \varrho_2}} \{T(\varrho_1(t_1), \varrho_2(t_1)) - T(\varrho_1(t_2), \varrho_2(t_2))\}, \tag{34}$$

where $T(\varrho_1, \varrho_2)$ is defined in the text below Eq. (24). The BLP measure has been related to the backflow of information, which can be quantified indeed in terms of the recovery of distinguishability. However, in order to quantify the amount of information recovered, it is much more sensible to use $\mathcal{N}_{\mathrm{MDR}}$ than integrating over all backflow in a process where information is fluctuating back and forth between system and environment. Of course, there is a price to pay. It is quite more expensive to compute $\mathcal{N}_{\mathrm{MDR}}$ than it is to compute $\mathcal{N}_{\mathrm{BLP}}$, because of the additional degrees of freedom, t_1 and t_2.

IV. NUMERICAL SIMULATIONS

In this section we apply different methods to characterize the (non-)Markovian dynamics of a generic open quantum system. The quantum process to be studied is obtained by numerical simulations of the Hamiltonian in Eq. (1) with the initial state of the environment taken as the maximally mixed state. This includes a Monte Carlo sampling of a random matrix ensemble. Therefore, the numerical data are contaminated by residual statistical fluctuations due to the finite size of the sample. We stress that residual fluctuations would be present in experimental situations also. The dimension of the Hilbert space of the environment is set to $N = 200$, and the sample size is fixed to $N_{\mathrm{sam}} = 2400$ unless otherwise stated.

In our model system, defined in Eq. (1), we can identify three different energy scales: the average level spacing in H_e (which is set equal to one), the spacing Δ between the two levels of the qubit, and the coupling strength λ between qubit and environment. In an effort to explore the properties of our model as thoroughly as possible, we consider a rectangular region in the parameter space (Δ, λ). For Δ, the interesting range reaches from values much smaller than the mean level spacing to values much larger, and thus we choose the limits $0.016 \leqslant \Delta \leqslant 16$, covering a range of three orders of magnitude. For λ, we choose the lower limit where λ is much smaller than the average level spacing in H_e, such that perturbation theory would be applicable for the Hamiltonian $H_e + \lambda V$. The upper limit, by contrast, is dictated by the requirement that our model reproduces the behavior of the random matrix model in the limit $N \to \infty$, in such a way that finite-size effects are still negligible. For that to hold, the spreading of eigenstates of $H_e + \lambda V$ expanded in the basis of H_e must be small compared to the spectral range of H_e. Both considerations lead us to the limits $1/32 \leqslant \lambda \leqslant 1/2$. A similar parameter range has been explored in Ref. [27].

In order to obtain reliable values for the two measures, we establish a finite ending time for the processes to be studied. At that time, the system will have relaxed so much that the remaining dynamics is unusable for any practical purposes. Our approach for finding a sensible definition for the ending time t_{End} is described in Sec. IV A. In Sec. IV B we present and discuss the results for three non-Markovianity measures. Moreover we select several representative parameter sets that are analyzed in detail in Sec. IV C. In particular, we study the dependence of the measures on the number of samples considered. The motivation is to understand the statistical significance of the results presented in Sec. IV B. At the end, this could be useful for identifying a NM measure which is accurate, robust, and significant. We finish this section by analyzing the local (in time) criteria for non-Markovianity in Sec. IV D. We consider divisibility and contractivity, via the corresponding inequalities (21) and (32). Both conditions are tested for the infinitesimal intermediate quantum map $\Lambda_{t+\varepsilon,t}$ as defined in Eq. (10) and examine carefully the usefulness of such kind of expression under statistical fluctuations.

A. Process ending time

For the NM measures to be considered below (Sec. IV B) it is essential to define an ending time t_{End} for the quantum process in question. However, two conflicting requirements arise. On the one hand, the ending time should be sufficiently large, such that the dynamics of the process is completely contained, but, on the other hand, it should also be sufficiently short, such that the contaminating contribution from residual statistical fluctuations remain small.

The quantum process studied here has the convenient property that if one chooses as initial state an eigenstate of σ_y, the system converges to the uniform mixture in the limit of long times. Along this process, the purity $P(t) = \mathrm{tr}[\varrho_c(t)^2]$ decays from $P(0) = 1$ to $P(\infty) = 1/2$. We choose the ending time for the process at that time, where the purity of $\Lambda_t[\varrho_c^{\mathrm{y}}]$ is equal to 0.51, which means that the purity has decayed to 2% above its minimum value. Of course, other values of the same order are equally possible, but they do not change the general results of our study.

In Fig. 1 we show the process ending time as a function of the parameters Δ and λ, color coded over the parameter space. While we use a linear scale for λ, Δ is varied on a log scale. The resulting ending time varies over several orders of magnitude, so we also use a log scale for the color mapping.

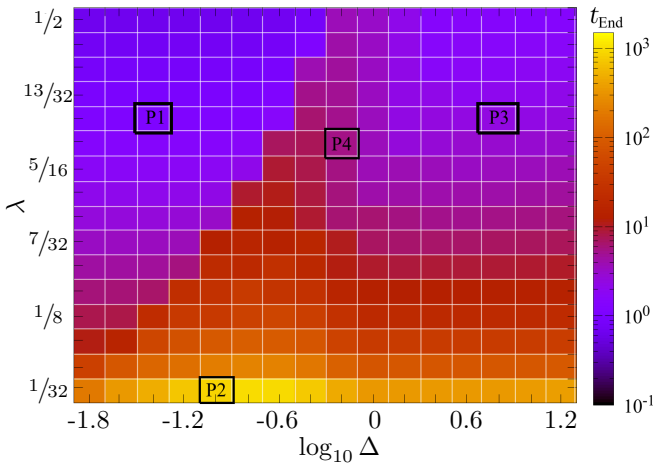

FIG. 1. Heat map of the process ending time t_{End} as a function of the qubit's energy splitting Δ and the strength of coupling with its environment λ.

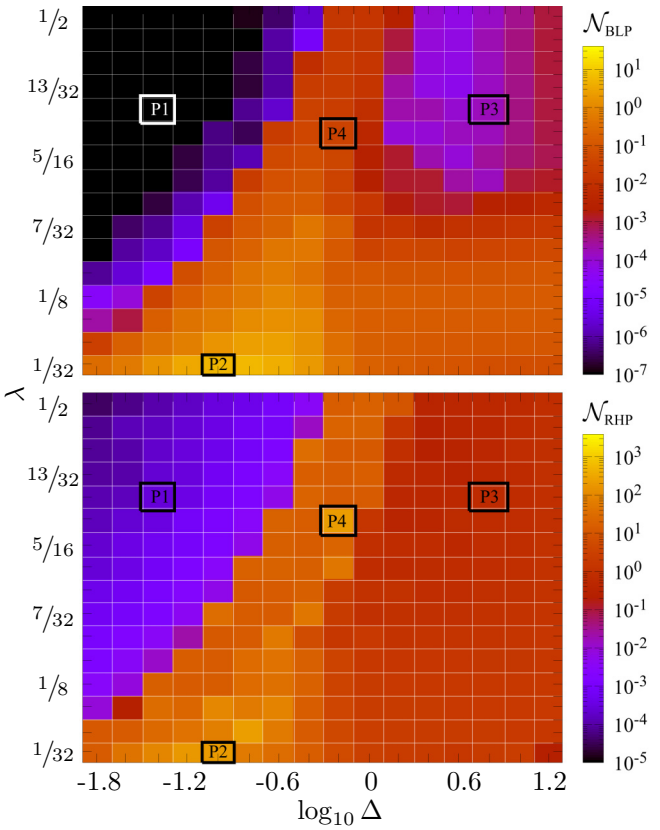

FIG. 2. BLP measure (upper panel) and RHP measure (lower panel) for non-Markovian dynamics as a function of Δ and λ. The parameter region considered is the same as in Fig. 1; again we use a log scale in the heat map representing the values of the NM measures. Both measures, defined in Eqs. (25) and (13), respectively, are taken at $t = t_{\mathrm{End}}$.

While λ increases, the t_{End} becomes smaller exponentially fast, since for large λ, the Fermi-golden-rule approximation applies [27]. It is, however, quite remarkable that for small λ, the largest t_{End} can be found near $\Delta = 0.16$, which is approximately equal to t_{H}^{-1}, where $t_{\mathrm{H}} = 2\pi$ is the Heisenberg time in the random matrix environment. In other words, at $\Delta = 0.16$ the period of the Rabi oscillation is equal to the Heisenberg time.

For all non Markovianity measures we choose $t = t_{\mathrm{End}}$ unless otherwise stated, and we shall thus drop the time dependence.

B. Three measures for non-Markovianity

Analyzing Fig. 2, we find that both measures reach smallest values shown in the upper left corner of the parameter space. Indeed, due to the following argument, we expect the quantum process to be at least close to Markovian in this region. The standard prescription for deriving a quantum master equation via the Born-Markov approximation consists in the following steps [37]: (1) couple the central system weakly to each of the many degrees of freedom in the environment (Born approximation), (2) let the number of degrees of freedom in the environment go to infinity, and (3) assume the environment correlation functions to decay almost instantaneously on the time scale of the reduced dynamics (Markov condition). In terms of level density and average local level spacing, conditions (1) and (2) lead to a wide range in energy with an exponentially high level density, which means that the perturbation strength will be large as compared to the level spacing. This regime is known as the Fermi-golden-rule regime [38]. Note that in this parameter region, $\Delta \ll 1$, which results in a slow system dynamics so that condition (3) is fulfilled.

By contrast, for sufficiently small coupling $\lambda < 7/32$ and not too small Δ, the dynamics is clearly NM. It is clear that in this region at least some of the conditions mentioned above are not fulfilled. The region of strongest NM behavior is around $\Delta \approx t_{\mathrm{H}}^{-1}$ and small values of λ.

An interesting area is in the upper right region of the NM maps in Fig. 2. There, the BLP measure of Eq. (25) tends to very small values, while the RHP measure, Eq. (13), remains constant. As explained at the end of Sec. III B, the RHP criterion is more restrictive than the BLP criterion, as it requires complete positivity and not just positivity for the intermediate maps. It is thus possible that a given quantum process is BLP Markovian but not RHP Markovian. Due to residual statistical fluctuations, a definite judgment is difficult.

Figure 3 shows $\mathcal{N}_{\mathrm{MDR}}(t)$ as defined in Eq. (34) up to the ending time $t = t_{\mathrm{End}}$ as a function of Δ and λ. Its behavior is more similar to $\mathcal{N}_{\mathrm{BLP}}$ than to $\mathcal{N}_{\mathrm{RHP}}$, which may be related to its common origin. Note though that the boundary between the regions of Markovian and strongly non-Markovian behavior is sharper. The region of strong NM is also somewhat larger, located in an area parallel to the M-NM boundary, at values for λ below 1/4, of about 12 blocks in size. Finally, note the region in the upper right corner. There the MDR measure leads to (relatively) lower values than the BLP measure, in distinction to the RHP measure, which reaches much larger values.

C. Robustness and convergence of the NM measures

In the previous section, we presented the results of three different measures for NM. For our model, we found a wide range of different behavior, depending on the choice of the

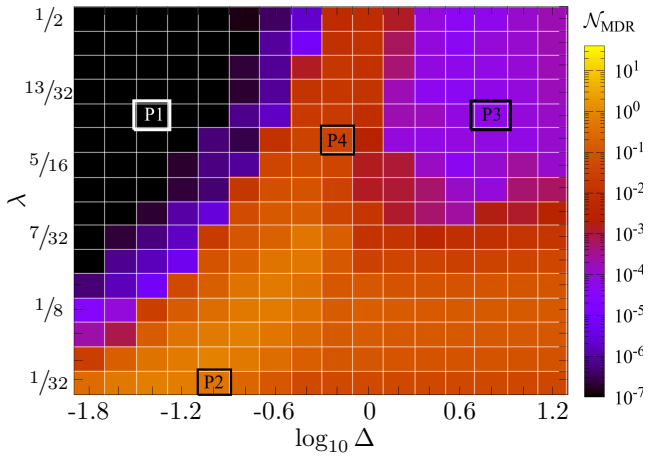

FIG. 3. Maximum distinguishability recovery (MDR). The quantity $\mathcal{N}_{\rm MDR}$ as defined in Eq. (34), plotted similarly to the previous two NM measures in Fig. 2.

parameters, Δ and λ. Here we study the robustness and accuracy of the measures in more detail. For that purpose we select three points in parameter space, where the behavior of the quantum process is quite different:

(1) Point P1 ($\Delta = 10^{-1.4}$, $\lambda = 3/8$), where the dynamics is Markovian, or at least very close to it.

(2) Point P2 ($\Delta = 0.1$, $\lambda = 1/32$), where it is maximally non-Markovian, according to the BLP measure.

(3) Point P3 ($\Delta = 10^{0.8}$, $\lambda = 3/8$), where the dynamics looks like being more NM according to RHP than according to BLP or MDR; compare the two heat maps in Fig. 2.

Finally, we select a additional fourth point for a later remark:

(4) Point P4 ($\Delta = 10^{-0.2}$, $\lambda = 11/32$).

Let us now discuss the numerical results. In Fig. 4 the NM measures are shown as a function of time. In other words, we compute the NM measures as if the quantum process would end at time t, instead of $t_{\rm End}$. It is clear from the definition of all three measures that they must be monotonously increasing: $\mathcal{N}(t_1) \geqslant \mathcal{N}(t_2)$ whenever $t_1 \geqslant t_2$.

For P1 (Markovian point; top panel), the RHP measure (blue line, triangles) increases continuously with time, even though it always remains rather small. The other two measures by contrast show only one increment at $t \approx 0.5$ and afterwards remain approximately constant around a value of 10^{-8}. This makes it difficult to decide unambiguously whether the process is Markovian or non-Markovian.

For P2 (strongly NM; middle panel), the RHP measure increases to very large values of the order of 10^{2}. The BLP measure also increases along the full time range up to values of the order 10^{0}, while the MDR measure quickly saturates at a value of the order of 10^{-1} (note that the MDR measure is by definition limited to values below one). The different behavior between BLP and MDR will be discussed below, where we consider the criteria for contractivity. In any case, all three measures clearly show the NM of the process.

For P3 the RHP measure increases continuously as in the previous cases, reaching values of the order of 10^{0}. By contrast, the other two measures, BLP and MDR remain

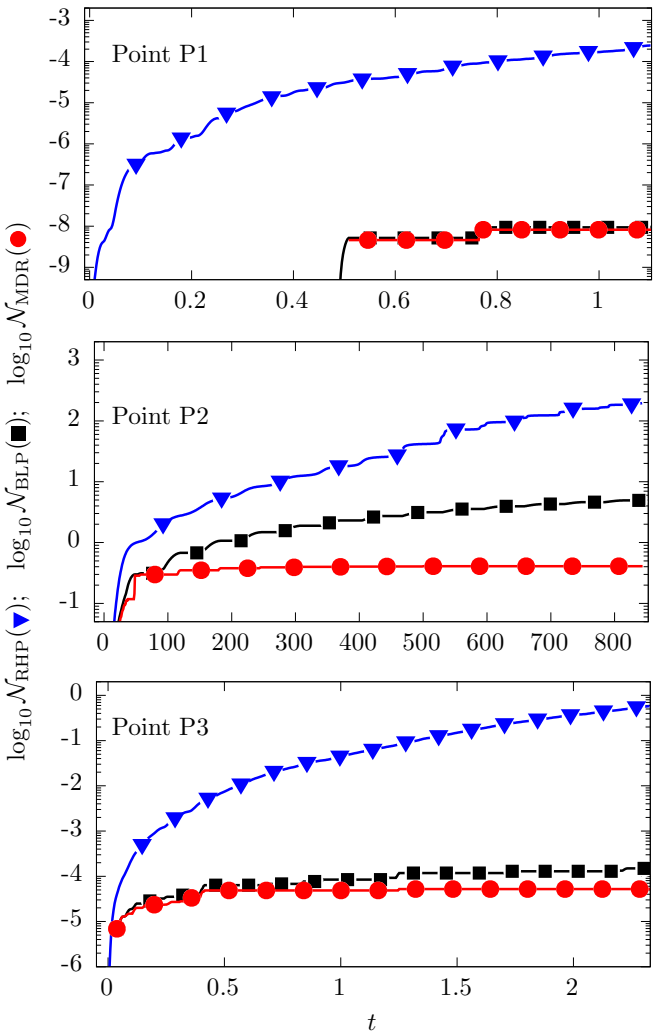

FIG. 4. NM measures for the three representative points P1, P2, and P3 (for details, see the main text), from the parametric plane as a function of time.

below a value of the order of 10^{-4}. This may hint towards the possibility that here the quantum process is P-divisible but not CP-divisible.

In Fig. 5 we plot the NM-measures versus the sample size, $N_{\rm sam}$, where we expect that the NM measures approach a limit value for $N_{\rm sam} \to \infty$, the true ensemble average. For point P1 (top panel), as the ensemble size increases, all measures tend algebraically to zero. For point P2 (middle panel) all measures converge to a finite values, whereas for point P3, the measures based on distinguishability seem to drop to zero, while the one based on divisibility attains a finite value. In other words, this result suggests that the dynamics is P-divisible but not CP-divisible at that point [35].

1. Environment size

The numerical results presented in this section were computed for $N_e = 200$ and are expected to show accurately the $N_e \to \infty$ limit. In fact, it can be shown that finite size effects of N_e may occur only at times of the order of $1/N_e$ or smaller (in units of the Heisenberg time). To give a quantitative

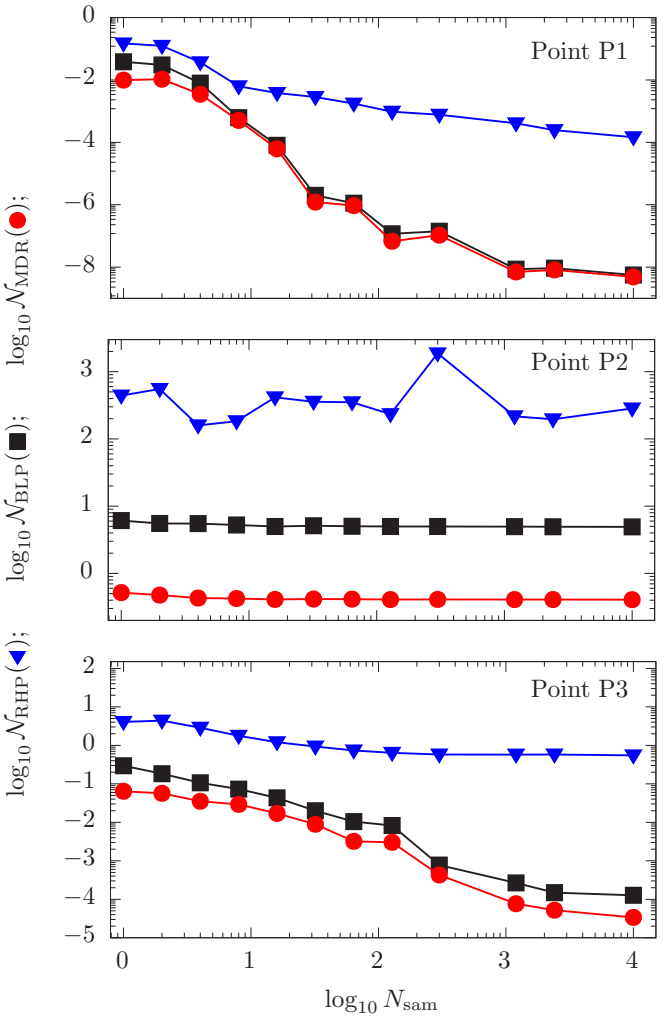

FIG. 5. NM measures for the same three representative points P1, P2, and P3, as in Fig. 4, as a function of the sample size.

answer, in the region $t < 0.06$ we saw relative differences not larger than 1% or 2% in the time-dependent quantities shown in our figures. We verified this by recalculating some of the observables for $N_e = 100$ and $N_e = 400$.

2. Nonequivalence of NM measures

A second interesting question is that of "quantitative equivalence." Two measures M_1, M_2 for a physical property may be called (quantitatively) equivalent, if and only if

$$M_1(A) < M_1(B) \Leftrightarrow M_2(A) < M_2(B),$$

for any two states A, B of some system. For example, if one thermometer (calibrated according to the empirical temperature M_1) finds that a body A is colder than a body B, any other thermometer (calibrated according to some different empirical temperature M_2) should find the same relation. Analyzing carefully our results in Fig. 2, we can indeed find pairs of points in parameter space, where the two NM measures $\mathcal{N}_{\rm RHP}$ and $\mathcal{N}_{\rm BLP}$ violate this condition. For instance, $\mathcal{N}_{\rm RHP}$ is clearly larger at P4 than at P2, while in the case of $\mathcal{N}_{\rm BLP}$ it is just the other way round.

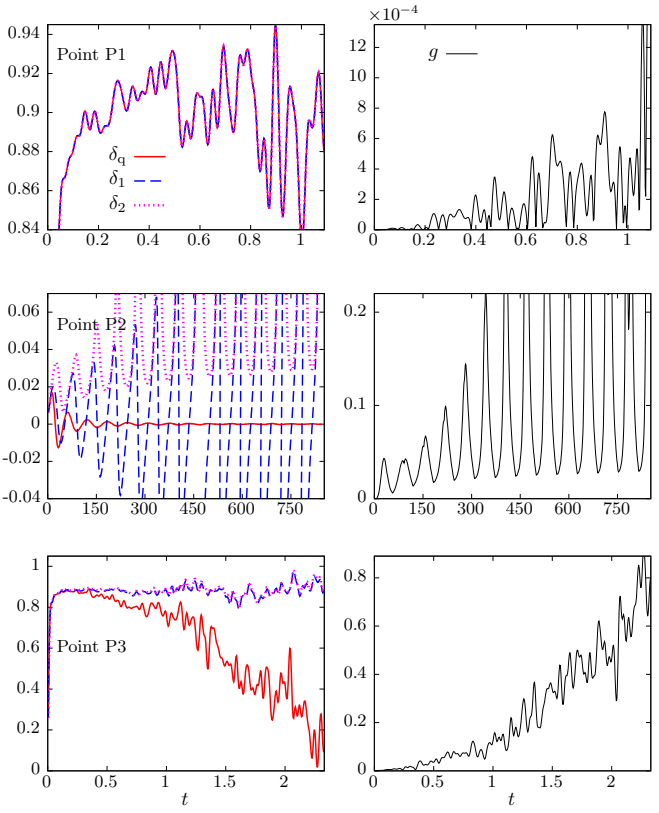

FIG. 6. Local divisibility criteria as a function of time for the well-known three points from the parametric plane. The left column shows the quantities, $\delta_{1,2,q}$ as defined in Eq. (20); the right column shows its corresponding function $g(t)$ as defined in Eq. (23). For the intermediate process to be divisible, the quantities on the left must fulfill $\delta_2 \leqslant \delta_q \leqslant \delta_1$, and the quantity on the right $g(t) = 0$. We present this figures for points P1 (top panel), P2 (middle panel), and P3 (bottom panel).

D. Time evolution of Markovianity criteria

Here we study the behavior of the two time-local criteria for non-Markovianity which are based on divisibility and contractivity, described in Sec. III.

For the divisibility, we consider the requirements given in Eq. (21) on the one hand, and the condition $g(t) = 0$ with $g(t)$ given in Eq. (12) on the other. While formally, both criteria are equivalent [see Eq. (23)], we will see that in the presence of experimental or statistical uncertainties, one might be easier to verify than the other. In Fig. 6 we present the aforementioned expressions for points P1, P2, and P3 for times ranging from zero to $t_{\rm End}$.

For point P1 (top two panels), we see that the inequalities are saturated, in the sense that $\delta_{1,2,q}$ are apparently all equal. Despite that, the function $g(t)$ is not identically equal to zero; however, it is small. The inequalities have allowed to correctly identify the point as Markovian, in agreement with the analysis of Fig. 5. In fact, for larger ensemble sizes the value of $g(t)$ diminishes.

The behavior of $\delta_{1,2,q}$ and $g(t)$ for point P2 can be seen in the middle panels of Fig. 6. Here the different curves corresponding to $\delta_{1,2,q}$ cross each other in a systematic and ordered fashion, indicating non-Markovianity beyond

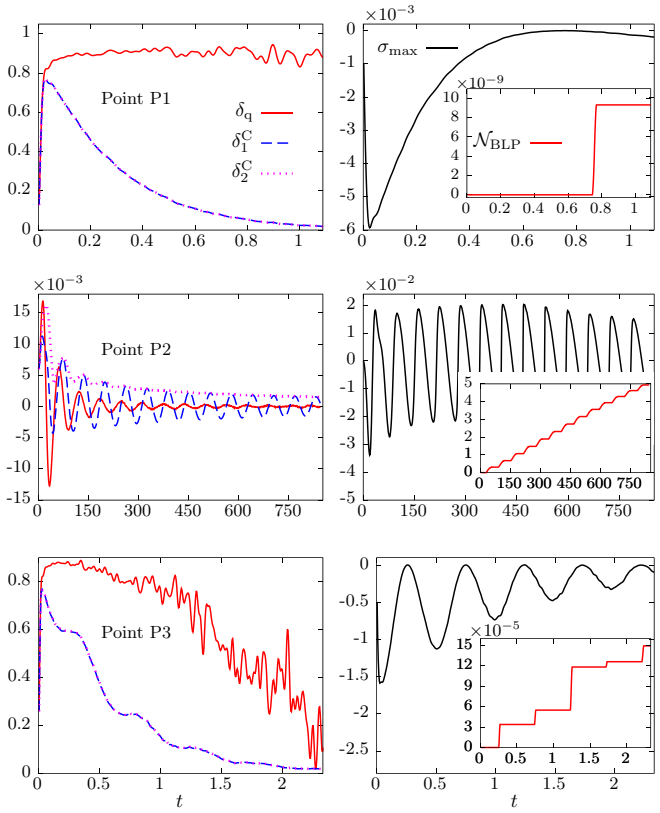

FIG. 7. Local contractivity criteria as a function of time. In the left figures, we plot the functions which characterize the channel to study how the conditions (32), $\delta_q \geqslant 0$ and $\delta_1^C \geqslant \delta_2^C$, are fulfilled or not. On the right we plot σ_{max} [Eq. (35)] to study how the measure builds with time, together with its integral (insets). Again, we study points P1, P2, and P3 in the top, middle, and bottom panels.

statistical fluctuations. This is also seen in the behavior of the corresponding $g(t)$, which oscillates regularly around values of the order of 0.1. Notice that we identified this point as displaying non-Markovian behavior, again with the aid of Fig. 5.

Finally, point P3 is studied in the lower panels of Fig. 6. We can see that the curve corresponding to δ_q is not between the ones corresponding to $\delta_{1,2}$. The conclusions are confirmed by the behavior of $g(t)$, where one finds striking fluctuations on top of a smooth curve which increases systematically as a function of time. Thus, according to the divisibility criterion, the system is non-Markovian, as concluded from the lower panel of Fig. 5.

In the case of the Markovianity measure based on the contractivity of the process, the condition $\sigma \leqslant 0$ translates to Eq. (32) for the channels here considered; see Fig. 7. For a given time t, a certain initial pair of states $\varrho_{1,2}^{(max)}$ will yield the maximum $\mathcal{N}_{BLP}(t)$ as defined in Eq. (25). For these states, one can calculate

$$\sigma_{max} = \sigma\left(\varrho_1^{(max)}, \varrho_2^{(max)}, t\right) \tag{35}$$

and see how the final value of the measure is built with time. Notice that σ_{max} is different from the derivative of $\mathcal{N}_{BLP}(t)$ [recall Eq. (25)] as for each ending time t, the states that maximize the quantifier are different, whereas in Eq. (35) we fix the ending time; however, for t equal to the ending time, they coincide.

On the top left panel we can see that Eq. (32) is apparently fulfilled during the whole process; however, since the two curves for δ_1^C and δ_2^C lie on top of each other, the inequality $\delta_1^C \geqslant \delta_2^C$ might be violated on a smaller scale. On the top right panel, we see that indeed the measure is close to zero; for $t < 0.7$ it is numerically zero and, afterwards, close to 10^{-8}. From this evidence, we arrive at the conclusion that the point is Markovian, with respect to contractivity, in agreement with the same case studied in Fig. 6.

The point P2 is analyzed in the middle panels. The function δ_q oscillates around zero with decreasing amplitude, while δ_2^C provides an upper bound for δ_1^C. Indeed, whenever this bound is saturated, δ_q has an node, and σ_{max} has a minimum, making the system "very Markovian." On the other hand, when the difference between δ_1^C and δ_2^C is largest, σ_{max} has a maximum, and the system becomes very non-Markovian. Thus, as can be seen on the right, σ_{max} oscillates regularly and with a relatively high amplitude around zero. The NM measure, $\mathcal{N}_{BLP}$, adds up the areas below the positive parts of $\sigma(t)$, which we expect to have a similar behavior as $\sigma_{max}(t)$, shown here. Therefore, the point P2 shows a genuine noncontractive behavior, and the dynamics is NM in this case.

The point P3 is analyzed in the bottom panels. All three functions δ_q and $\delta_{1,2}^C$ display a similar behavior as for point P1, but for δ_q we observe stronger statistical fluctuations. In this case, however, σ_{max} oscillates and has a maximum in 0. The measure picks up small statistical fluctuations which diminish as we increase the sample size and may therefore be regarded as spurious. We can conclude that the process for point P3 is contractive, in agreement with previous conclusions.

The criteria provided in Eqs. (21) and (32), indeed, provide a useful tool to understand if a certain nonzero value for one of the NM measures should be regarded as statistically significant or not. In some cases it is helpful to analyze the behavior of the measures under variation of the sample size in order to arrive at the correct decision.

V. CONCLUSIONS

In this article we studied a qubit coupled to a generic environment modeled by random matrices. The model Hamiltonian contains a factorizable interaction between qubit and environment, and provides the qubit with an internal dynamics perpendicular (in the Bloch representation) to the one induced by the interaction. This induces a channel structure for which we were able to derive analytical conditions for several criteria of Markovianity. In spite of its simplicity, the model displays rich dynamics in the qubit, beyond pure depolarization or dephasing.

We then applied the criteria to determine for which parameters the model yield Markovian dynamics in the qubit. We found several difficulties with verifying Markovianity criteria for the numerical data, which we expect to appear also in real experimental situations. Fluctuations due to noise and/or due to finite sample sizes may contribute notably to the finite value of a non-Markovianity measure and thereby suggest non-Markovian behavior, whereas the clean system really is Markovian. An analysis like the present one, where

the ensemble size is increased such that residual fluctuations diminish, eventually reveals the true behavior.

ACKNOWLEDGMENTS

Support by projects CONACyT 285754, UNAM-PAPIIT IG100518, Benemérita Universidad Autónoma de Puebla (BUAP) PRODEP 511-6/2019-4354, and CONACyT 220624-CB is acknowledged.

APPENDIX A: BORN SERIES

In this Appendix, we prove that the quantum channel, describing the dynamics of the qubit under coupling to the RMT environment, has the form of an X state [39] as postulated in Eq. (7). For doing so, we use the entire expansion of the evolution of system and environment in a Born series. We consider the more general case of an arbitrary mixed initial state ϱ_e in the environment, and only at the end specialize to the case $\varrho_e = \mathbb{1}/N_e$.

In the interaction picture, a solution to the Hamiltonian

$$H_\lambda = \frac{\Delta}{2}\,\sigma_z \otimes \mathbb{1} + \mathbb{1} \otimes H_e + \lambda\,\sigma_x \otimes V_e$$

can be written as

$$\Psi(t) = U_0(t)\,\chi(t): \quad i\hbar\partial_t\,\chi(t) = \lambda U_0(t)^\dagger\,\sigma_x \otimes V_e\,U_0(t)\chi(t),$$
$$U_0(t) = e^{-i\frac{\Delta}{2}\sigma_z t} \otimes e^{-iH_e t}.$$

Here we stick to the convention chosen in the main part of this paper, where the time variable t measures time in units of the Heisenberg time, which results in $\hbar = 1$. The echo operator $M(t)$ describes the evolution of the state $\chi(t)$, such that $\chi(t) = M(t)\,\chi(0)$. In the original Schrödinger picture, it thus holds:

$$\Psi(t) = U_0(t)\,M(t)\,\Psi(0), \quad M(t) = U_0(t)^\dagger\,U(t).$$

As a formal solution of the evolution equation in the interaction picture, the echo operator fulfills the following integral equation:

$$\begin{aligned} M(t) &= M(0) - i\lambda\int_0^t d\tau\;\tilde{\sigma}_x(\tau)\otimes\tilde{V}_e(\tau)\,M(\tau) \\ &= \sum_{k=0}^{\infty}(-i\lambda)^k\int\cdots\int_{t>\tau_k>\ldots>\tau_1>0} d\tau_k\cdots d\tau_1 \\ &\quad\times\begin{pmatrix}0 & A(\tau_k)\\ A(\tau_k)^\dagger & 0\end{pmatrix}\cdots\begin{pmatrix}0 & A(\tau_1)\\ A(\tau_1)^\dagger & 0\end{pmatrix}. \end{aligned} \tag{A1}$$

Here the second line represents the afore mentioned Born series, where the interaction has been written in block-matrix notation:

$$\tilde{\sigma}_x(\tau)\otimes\tilde{V}_e(\tau) = \begin{pmatrix}0 & e^{i\Delta\tau}\,\tilde{V}_e(\tau)\\ e^{-i\Delta\tau}\,\tilde{V}_e & 0\end{pmatrix} = \begin{pmatrix}0 & A(\tau)\\ A(\tau)^\dagger & 0\end{pmatrix}.$$

Here we will calculate the average of $\tilde{\varrho}(t) = M(t)\,\varrho_c \otimes \varrho_e\,M(t)^\dagger$, with respect to the random matrix ensemble for V_e. This defines the quantum map Λ_t as

$$\begin{aligned} \Lambda_t : \varrho_c(0) \to \varrho_c(t) &= \mathrm{tr}_e[U(t)\,\varrho_c(0)\otimes\varrho_e\,U(t)^\dagger] \\ &= \begin{pmatrix}e^{-i\Delta t/2} & 0\\ 0 & e^{i\Delta t/2}\end{pmatrix}\mathrm{tr}_e[\tilde{\varrho}(t)] \\ &\quad\times\begin{pmatrix}e^{i\Delta t/2} & 0\\ 0 & e^{-i\Delta t/2}\end{pmatrix}, \end{aligned} \tag{A2}$$

and thereby its Choi-matrix representation, in Eq. (7). Below, we will also consider this quantum map in the interaction picture, defined as

$$\tilde{\Lambda}_t : \varrho_c(0) \to \tilde{\varrho}_c(t) = \mathrm{tr}_e[\tilde{\varrho}(t)]. \tag{A3}$$

1. Simplified notation

For our purpose, it is convenient to introduce the following more compact notation for the multidimensional time integrals:

$$\mathcal{I}^0(\boldsymbol{\tau}) = 1, \quad \mathcal{I}^1(\boldsymbol{\tau}) = \mathcal{I}(\tau) = \int_0^t d\tau, \quad \mathcal{I}^2(\boldsymbol{\tau}) = \mathcal{I}(\tau_2,\tau_1) = \int_{t>\tau_2>\tau_1>0} d^2\boldsymbol{\tau} = \int_{t>\tau_2>\tau_1>0} d\tau_2\,d\tau_1,$$
$$\mathcal{I}^k(\boldsymbol{\tau}) = \int_{t>\tau_k>\ldots>\tau_1>0} d\tau_k\cdots d\tau_1. \tag{A4}$$

Note that we enumerate the different time variables from smallest to largest starting at the time closest to zero. Next, we will introduce an independent notation for the integrands. Let us consider the case of an even number of product terms, first:

$$\prod_{j=1}^{2k}\begin{pmatrix}0 & A(\tau_j)\\ A(\tau_j)^\dagger & 0\end{pmatrix} = \begin{pmatrix}P_{2k}(\boldsymbol{\tau}) & 0\\ 0 & Q_{2k}(\boldsymbol{\tau})\end{pmatrix}, \quad A(\tau) = e^{i\Delta\tau}\,\tilde{V}_e(\tau), \quad A(\tau)^\dagger = e^{-i\Delta\tau}\,\tilde{V}_e(\tau) = e^{-2i\Delta\tau}\,A(\tau),$$

since $\tilde{V}_e(\tau)$ is Hermitian. Note that the product terms on the left-hand side of the first equation, must be ordered according to decreasing time arguments, just as in Eq. (A1). From an explicit computation we find

$$P_{2k}(\boldsymbol{\tau}) = A(\tau_{2k})\,A(\tau_{2k-1})^\dagger\,A(\tau_{2k-2})\,A(\tau_{2k-3})^\dagger\;\cdots\;A(\tau_2)\,A(\tau_1)^\dagger = \exp\left[-i\Delta\sum_{m=1}^{2k}(-1)^m\,\tau_m\right]\prod_{m=1}^{2k}\tilde{V}(\tau_m),$$
$$Q_{2k}(\boldsymbol{\tau}) = A(\tau_{2k})^\dagger\,A(\tau_{2k-1})\,A(\tau_{2k-2})^\dagger\,A(\tau_{2k-3})\;\cdots\;A(\tau_2)^\dagger\,A(\tau_1) = \exp\left[i\Delta\sum_{m=1}^{2k}(-1)^m\,\tau_m\right]\prod_{m=1}^{2k}\tilde{V}(\tau_m). \tag{A5}$$

Note that the product terms must be ordered such that time increases from right to left. For an odd number of terms:

$$\prod_{j=1}^{2k+1}\begin{pmatrix}0 & A(\tau_j)\\ A(\tau_j)^\dagger & 0\end{pmatrix}=\begin{pmatrix}0 & A(\tau_{2k+1})\\ A(\tau_{2k+1})^\dagger & 0\end{pmatrix}\begin{pmatrix}P_{2k}(\boldsymbol{\tau}) & 0\\ 0 & Q_{2k}(\boldsymbol{\tau})\end{pmatrix}=\begin{pmatrix}0 & A(\tau_{2k+1})\,Q_{2k}(\boldsymbol{\tau})\\ A(\tau_{2k+1})^\dagger\,P_{2k}(\boldsymbol{\tau}) & 0\end{pmatrix}$$
$$=\begin{pmatrix}0 & Q_{2k+1}(\boldsymbol{\tau})\\ P_{2k+1}(\boldsymbol{\tau}) & 0\end{pmatrix}. \tag{A6}$$

With this, we can write for the echo operator

$$M(t)=\sum_{k=0}^{\infty}\left\{(-i\lambda)^{2k}\,\mathcal{I}^{2k}(\boldsymbol{\tau})\begin{pmatrix}P_{2k}(\boldsymbol{\tau}) & 0\\ 0 & Q_{2k}(\boldsymbol{\tau})\end{pmatrix}+(-i\lambda)^{2k+1}\,\mathcal{I}^{2k+1}(\boldsymbol{\tau})\begin{pmatrix}0 & Q_{2k+1}(\boldsymbol{\tau})\\ P_{2k+1}(\boldsymbol{\tau}) & 0\end{pmatrix}\right\}. \tag{A7}$$

2. Ensemble averaged quantum channel

Averaging over the random matrix V_e implies that only such terms survive that contain an even power of matrices $A(\tau_k)$ and $A(\sigma_{k'})$. This means that the indices of summation must either be both even or both odd. Therefore,

$$\begin{aligned}\tilde{\varrho}(t)=&\sum_{k,k'=0}^{\infty}(-i\lambda)^{2k}\,\mathcal{I}^{2k}(\boldsymbol{\tau})\begin{pmatrix}P_{2k}(\boldsymbol{\tau}) & 0\\ 0 & Q_{2k}(\boldsymbol{\tau})\end{pmatrix}\varrho_c\otimes\varrho_e\,(i\lambda)^{2k'}\,\mathcal{I}^{2k'}(\boldsymbol{\tau})\begin{pmatrix}P_{2k'}(\boldsymbol{\tau})^\dagger & 0\\ 0 & Q_{2k'}(\boldsymbol{\tau})^\dagger\end{pmatrix}\\
&+\sum_{k,k'=0}^{\infty}(-i\lambda)^{2k+1}\,\mathcal{I}^{2k+1}(\boldsymbol{\tau})\begin{pmatrix}0 & Q_{2k+1}(\boldsymbol{\tau})\\ P_{2k+1}(\boldsymbol{\tau}) & 0\end{pmatrix}\varrho_c\otimes\varrho_e\,(i\lambda)^{2k'+1}\,\mathcal{I}^{2k'+1}(\boldsymbol{\tau})\begin{pmatrix}0 & Q_{2k'+1}(\boldsymbol{\tau})^\dagger\\ P_{2k'+1}(\boldsymbol{\tau})^\dagger & 0\end{pmatrix}\\
=&\sum_{k,k'=0}^{\infty}(-\lambda^2)^{k+k'}\left\{\mathcal{I}^{2k}(\boldsymbol{\tau})\,\mathcal{I}^{2k'}(\boldsymbol{\sigma})\begin{pmatrix}P_{2k}(\boldsymbol{\tau}) & 0\\ 0 & Q_{2k}(\boldsymbol{\tau})\end{pmatrix}\varrho_c\otimes\varrho_e\begin{pmatrix}P_{2k'}(\boldsymbol{\sigma})^\dagger & 0\\ 0 & Q_{2k'}(\boldsymbol{\sigma})^\dagger\end{pmatrix}\right.\\
&\left.+\lambda^2\,\mathcal{I}^{2k+1}(\boldsymbol{\tau})\,\mathcal{I}^{2k'+1}(\boldsymbol{\sigma})\begin{pmatrix}0 & Q_{2k+1}(\boldsymbol{\tau})\\ P_{2k+1}(\boldsymbol{\tau}) & 0\end{pmatrix}\varrho_c\otimes\varrho_e\begin{pmatrix}0 & Q_{2k'+1}(\boldsymbol{\sigma})^\dagger\\ P_{2k'+1}(\boldsymbol{\sigma})^\dagger & 0\end{pmatrix}\right\}.\end{aligned} \tag{A8}$$

For the quantum channel in the interaction picture, Eq. (A3), it is now easily verified that

$$\begin{aligned}\tilde{\Lambda}_t[\,|0\rangle\langle 0|\,]=&\sum_{k,k'=0}^{\infty}(-\lambda^2)^{k+k'}\,\mathrm{tr}_e\left\{\mathcal{I}^{2k}(\boldsymbol{\tau})\,\mathcal{I}^{2k'}(\boldsymbol{\sigma})\begin{pmatrix}P_{2k}(\boldsymbol{\tau}) & 0\\ 0 & Q_{2k}(\boldsymbol{\tau})\end{pmatrix}\begin{pmatrix}\varrho_e & 0\\ 0 & 0\end{pmatrix}\begin{pmatrix}P_{2k'}(\boldsymbol{\sigma})^\dagger & 0\\ 0 & Q_{2k'}(\boldsymbol{\sigma})^\dagger\end{pmatrix}\right.\\
&\left.+\lambda^2\,\mathcal{I}^{2k+1}(\boldsymbol{\tau})\,\mathcal{I}^{2k'+1}(\boldsymbol{\sigma})\begin{pmatrix}0 & Q_{2k+1}(\boldsymbol{\tau})\\ P_{2k+1}(\boldsymbol{\tau}) & 0\end{pmatrix}\begin{pmatrix}\varrho_e & 0\\ 0 & 0\end{pmatrix}\begin{pmatrix}0 & Q_{2k'+1}(\boldsymbol{\sigma})^\dagger\\ P_{2k'+1}(\boldsymbol{\sigma})^\dagger & 0\end{pmatrix}\right\}\\
=&\sum_{k,k'=0}^{\infty}(-\lambda^2)^{k+k'}\left\{\mathcal{I}^{2k}(\boldsymbol{\tau})\,\mathcal{I}^{2k'}(\boldsymbol{\sigma})\begin{pmatrix}P_{2k}(\boldsymbol{\tau})\,\varrho_e\,P_{2k'}(\boldsymbol{\sigma})^\dagger & 0\\ 0 & 0\end{pmatrix}\right.\\
&\left.+\lambda^2\,\mathcal{I}^{2k+1}(\boldsymbol{\tau})\,\mathcal{I}^{2k'+1}(\boldsymbol{\sigma})\begin{pmatrix}0 & 0\\ 0 & P_{2k+1}(\boldsymbol{\tau})\,\varrho_e\,Q_{2k'+1}(\boldsymbol{\sigma})^\dagger\end{pmatrix}\right\}.\end{aligned} \tag{A9}$$

This and Eq. (A2) then show that $\Lambda_t[|0\rangle\langle 0|]$ is indeed of the form postulated in Eq. (7), and it yields the following expressions for $r(t)$:

$$r(t)=\sum_{k,k'=0}^{\infty}(-\lambda^2)^{k+k'}\,\mathcal{I}^{2k}(\boldsymbol{\tau})\,\mathcal{I}^{2k'}(\boldsymbol{\sigma})\,\mathrm{tr}[P_{2k}(\boldsymbol{\tau})\,\varrho_e\,P_{2k'}(\boldsymbol{\sigma})^\dagger], \tag{A10}$$

$$1-r(t)=-\sum_{k,k'=0}^{\infty}(-\lambda^2)^{k+k'+1}\,\mathcal{I}^{2k+1}(\boldsymbol{\tau})\,\mathcal{I}^{2k'+1}(\boldsymbol{\sigma})\,\mathrm{tr}[P_{2k+1}(\boldsymbol{\tau})\,\varrho_e\,Q_{2k'+1}(\boldsymbol{\sigma})^\dagger]. \tag{A11}$$

The second equation results from the fact that the reduced evolution of the qubit conserves the trace. Naturally, it is difficult to prove this directly, from the expressions derived here. Let us now consider $\Lambda_t[|1\rangle\langle 1|]$. In this case, as in the previous one, $\Lambda_t[|1\rangle\langle 1|]=\tilde{\Lambda}_t[|1\rangle\langle 1|]$, and we find

$$\begin{aligned}\Lambda_t[|1\rangle\langle 1|]=&\sum_{k,k'=0}^{\infty}(-\lambda^2)^{k+k'}\,\mathrm{tr}_e\left\{\mathcal{I}^{2k}(\boldsymbol{\tau})\,\mathcal{I}^{2k'}(\boldsymbol{\sigma})\begin{pmatrix}P_{2k}(\boldsymbol{\tau}) & 0\\ 0 & Q_{2k}(\boldsymbol{\tau})\end{pmatrix}\begin{pmatrix}0 & 0\\ 0 & \varrho_e\end{pmatrix}\begin{pmatrix}P_{2k'}(\boldsymbol{\sigma})^\dagger & 0\\ 0 & Q_{2k'}(\boldsymbol{\sigma})^\dagger\end{pmatrix}\right.\\
&\left.+\lambda^2\,\mathcal{I}^{2k+1}(\boldsymbol{\tau})\,\mathcal{I}^{2k'+1}(\boldsymbol{\sigma})\begin{pmatrix}0 & Q_{2k+1}(\boldsymbol{\tau})\\ P_{2k+1}(\boldsymbol{\tau}) & 0\end{pmatrix}\begin{pmatrix}0 & 0\\ 0 & \varrho_e\end{pmatrix}\begin{pmatrix}0 & Q_{2k'+1}(\boldsymbol{\sigma})^\dagger\\ P_{2k'+1}(\boldsymbol{\sigma})^\dagger & 0\end{pmatrix}\right\}\end{aligned}$$

$$= \sum_{k,k'=0}^{\infty} (-\lambda^2)^{k+k'} \left\{ \mathcal{I}^{2k}(\boldsymbol{\tau})\, \mathcal{I}^{2k'}(\boldsymbol{\sigma}) \begin{pmatrix} 0 & 0 \\ 0 & Q_{2k}(\boldsymbol{\tau})\, \varrho_e\, Q_{2k'}(\boldsymbol{\sigma})^\dagger \end{pmatrix} \right.$$
$$\left. + \lambda^2\, \mathcal{I}^{2k+1}(\boldsymbol{\tau})\, \mathcal{I}^{2k'+1}(\boldsymbol{\sigma}) \begin{pmatrix} Q_{2k+1}(\boldsymbol{\tau})\, \varrho_e\, P_{2k'+1}(\boldsymbol{\sigma})^\dagger & 0 \\ 0 & 0 \end{pmatrix} \right\} = \begin{pmatrix} 1-\tilde{r}(t) & 0 \\ 0 & \tilde{r}(t) \end{pmatrix}. \tag{A12}$$

Again, the resulting qubit state is diagonal; however, unless we specialize to the case $\varrho_e = \mathbb{1}/N$, the function $\tilde{r}(t)$ is different from $r(t)$ corresponding to the previous case:

$$\tilde{r}(t) = \sum_{k,k'=0}^{\infty} (-\lambda^2)^{k+k'}\, \mathcal{I}^{2k}(\boldsymbol{\tau})\, \mathcal{I}^{2k'}(\boldsymbol{\sigma})\, \mathrm{tr}[Q_{2k}(\boldsymbol{\tau})\, \varrho_e\, Q_{2k'}(\boldsymbol{\sigma})^\dagger],$$
$$1-\tilde{r}(t) = -\sum_{k,k'=0}^{\infty} (-\lambda^2)^{k+k'+1}\, \mathcal{I}^{2k+1}(\boldsymbol{\tau})\, \mathcal{I}^{2k'+1}(\boldsymbol{\sigma})\, \mathrm{tr}[Q_{2k+1}(\boldsymbol{\tau})\, \varrho_e\, P_{2k'+1}(\boldsymbol{\sigma})^\dagger]. \tag{A13}$$

We continue with the off-diagonal blocks of the Choi-matrix representation of the quantum channel:

$$\tilde{\Lambda}_t[|1\rangle\langle 0|] = \sum_{k,k'=0}^{\infty} (-\lambda^2)^{k+k'}\, \mathrm{tr}_e \left\{ \mathcal{I}^{2k}(\boldsymbol{\tau})\, \mathcal{I}^{2k'}(\boldsymbol{\sigma}) \begin{pmatrix} P_{2k}(\boldsymbol{\tau}) & 0 \\ 0 & Q_{2k}(\boldsymbol{\tau}) \end{pmatrix} \begin{pmatrix} 0 & 0 \\ \varrho_e & 0 \end{pmatrix} \begin{pmatrix} P_{2k'}(\boldsymbol{\sigma})^\dagger & 0 \\ 0 & Q_{2k'}(\boldsymbol{\sigma})^\dagger \end{pmatrix} \right.$$
$$\left. + \lambda^2\, \mathcal{I}^{2k+1}(\boldsymbol{\tau})\, \mathcal{I}^{2k'+1}(\boldsymbol{\sigma}) \begin{pmatrix} 0 & Q_{2k+1}(\boldsymbol{\tau}) \\ P_{2k+1}(\boldsymbol{\tau}) & 0 \end{pmatrix} \begin{pmatrix} 0 & 0 \\ \varrho_e & 0 \end{pmatrix} \begin{pmatrix} 0 & Q_{2k'+1}(\boldsymbol{\sigma})^\dagger \\ P_{2k'+1}(\boldsymbol{\sigma})^\dagger & 0 \end{pmatrix} \right\}$$
$$= \sum_{k,k'=0}^{\infty} (-\lambda^2)^{k+k'} \left\{ \mathcal{I}^{2k}(\boldsymbol{\tau})\, \mathcal{I}^{2k'}(\boldsymbol{\sigma}) \begin{pmatrix} 0 & 0 \\ Q_{2k}(\boldsymbol{\tau})\, \varrho_e\, P_{2k'}(\boldsymbol{\sigma})^\dagger & 0 \end{pmatrix} \right.$$
$$\left. + \lambda^2\, \mathcal{I}^{2k+1}(\boldsymbol{\tau})\, \mathcal{I}^{2k'+1}(\boldsymbol{\sigma}) \begin{pmatrix} 0 & Q_{2k+1}(\boldsymbol{\tau})\, \varrho_e\, Q_{2k'+1}(\boldsymbol{\sigma})^\dagger \\ 0 & 0 \end{pmatrix} \right\}. \tag{A14}$$

This result confirms again the general X-state structure of the Choi representation of our quantum channel. In terms of the parametrization in Eq. (7), we find

$$z_1(t) = e^{i\Delta t} \sum_{k,k'=0}^{\infty} (-\lambda^2)^{k+k'}\, \mathcal{I}^{2k}(\boldsymbol{\tau})\, \mathcal{I}^{2k'}(\boldsymbol{\sigma})\, \mathrm{tr}[Q_{2k}(\boldsymbol{\tau})\, \varrho_e\, P_{2k'}(\boldsymbol{\sigma})^\dagger],$$
$$z_2(t)^* = e^{-i\Delta t} \sum_{k,k'=0}^{\infty} (-\lambda^2)^{k+k'}\, \lambda^2\, \mathcal{I}^{2k+1}(\boldsymbol{\tau})\, \mathcal{I}^{2k'+1}(\boldsymbol{\sigma})\, \mathrm{tr}[Q_{2k+1}(\boldsymbol{\tau})\, \varrho_e\, Q_{2k'+1}(\boldsymbol{\sigma})^\dagger], \tag{A15}$$

where the phases $e^{\pm i\Delta t}$ arise from returning to the Schrödinger picture, according to Eq. (A2). Finally,

$$\tilde{\Lambda}_t[|0\rangle\langle 1|] = \sum_{k,k'=0}^{\infty} (-\lambda^2)^{k+k'}\, \mathrm{tr}_e \left\{ \mathcal{I}^{2k}(\boldsymbol{\tau})\, \mathcal{I}^{2k'}(\boldsymbol{\sigma}) \begin{pmatrix} P_{2k}(\boldsymbol{\tau}) & 0 \\ 0 & Q_{2k}(\boldsymbol{\tau}) \end{pmatrix} \begin{pmatrix} 0 & \varrho_e \\ 0 & 0 \end{pmatrix} \begin{pmatrix} P_{2k'}(\boldsymbol{\sigma})^\dagger & 0 \\ 0 & Q_{2k'}(\boldsymbol{\sigma})^\dagger \end{pmatrix} \right.$$
$$\left. + \lambda^2\, \mathcal{I}^{2k+1}(\boldsymbol{\tau})\, \mathcal{I}^{2k'+1}(\boldsymbol{\sigma}) \begin{pmatrix} 0 & Q_{2k+1}(\boldsymbol{\tau}) \\ P_{2k+1}(\boldsymbol{\tau}) & 0 \end{pmatrix} \begin{pmatrix} 0 & \varrho_e \\ 0 & 0 \end{pmatrix} \begin{pmatrix} 0 & Q_{2k'+1}(\boldsymbol{\sigma})^\dagger \\ P_{2k'+1}(\boldsymbol{\sigma})^\dagger & 0 \end{pmatrix} \right\}$$
$$= \sum_{k,k'=0}^{\infty} (-\lambda^2)^{k+k'} \left\{ \mathcal{I}^{2k}(\boldsymbol{\tau})\, \mathcal{I}^{2k'}(\boldsymbol{\sigma}) \begin{pmatrix} 0 & P_{2k}(\boldsymbol{\tau})\, \varrho_e\, Q_{2k'}(\boldsymbol{\sigma})^\dagger \\ 0 & 0 \end{pmatrix} \right.$$
$$\left. + \lambda^2\, \mathcal{I}^{2k+1}(\boldsymbol{\tau})\, \mathcal{I}^{2k'+1}(\boldsymbol{\sigma}) \begin{pmatrix} 0 & 0 \\ P_{2k+1}(\boldsymbol{\tau})\, \varrho_e\, P_{2k'+1}(\boldsymbol{\sigma})^\dagger & 0 \end{pmatrix} \right\}. \tag{A16}$$

For any Hermiticity-conserving linear map, the Choi representation itself must be Hermitian, in particular also for our quantum channel, as can be seen from its definition in terms of the reduced dynamics in Eq. (2). This implies that

$$z_1(t)^* = e^{-i\Delta t} \sum_{k,k'=0}^{\infty} (-\lambda^2)^{k+k'}\, \mathcal{I}^{2k}(\boldsymbol{\tau})\, \mathcal{I}^{2k'}(\boldsymbol{\sigma})\, \mathrm{tr}[P_{2k}(\boldsymbol{\tau})\, \varrho_e\, Q_{2k'}(\boldsymbol{\sigma})^\dagger],$$
$$z_2(t) = e^{i\Delta t} \sum_{k,k'=0}^{\infty} (-\lambda^2)^{k+k'}\, \lambda^2\, \mathcal{I}^{2k+1}(\boldsymbol{\tau})\, \mathcal{I}^{2k'+1}(\boldsymbol{\sigma})\, \mathrm{tr}[P_{2k+1}(\boldsymbol{\tau})\, \varrho_e\, P_{2k'+1}(\boldsymbol{\sigma})^\dagger]. \tag{A17}$$

In the case of $z_1(t)$ the equivalence of the Eqs. (A15) and (A17) is rather obvious. One simply has to exchange the variable names k and k' along with $\boldsymbol{\tau}$ and $\boldsymbol{\sigma}$. In the case of $z_2(t)$, we do not see any simple way of proving the equivalence in terms of the present approach.

3. Collecting results for the case $\varrho_e = \mathbb{1}/N$

From the considerations in the previous paragraph, we found that the Choi-matrix representation of the quantum channel defined by the Eqs. (2) and (A2) is given by

$$C_{\Lambda_t} = \begin{pmatrix} r & 0 & 0 & z_1^* \\ 0 & 1-r & z_2 & 0 \\ 0 & z_2^* & 1-\tilde{r} & 0 \\ z_1 & 0 & 0 & \tilde{r} \end{pmatrix}.$$

The general X-state structure (i.e., all the zeros in this matrix) follows directly from the considerations in this section. For simplicity we omitted the time argument in this representation. The functions $r(t)$, $z_1(t)$, $z_2(t)$, and $\tilde{r}(t)$ are as defined above. Some of the dependencies between these matrix elements could not be proven within our derivation but are valid due to elementary properties of the evolution equation (2). This is the case for trace conservation (diagonal blocks) and Hermiticity (off-diagonal blocks).

As a last point, we show that for $\varrho_e = \mathbb{1}/N_e$, it holds that $r(t) = \tilde{r}(t)$. In this case, and for $\varrho_e(0) = \mathbb{1}_2$, we find from Eq. (2):

$$\Lambda_t[\mathbb{1}] = \frac{1}{N_e}\,\mathrm{tr}_e\left[e^{-iH_\lambda t}\, e^{iH_\lambda t}\right] = \mathbb{1}. \tag{A18}$$

This means that no matte if we perform an ensemble average or not, the resulting quantum channel is unital (it maps the identity onto itself). This in turn implies

$$\begin{aligned} \Lambda_t[\mathbb{1}] &= \Lambda_t[|0\rangle\langle 0|] + \Lambda_t[|1\rangle\langle 1|] \\ &= \begin{pmatrix} r(t) & 0 \\ 0 & 1-r(t) \end{pmatrix} + \begin{pmatrix} 1-\tilde{r}(t) & 0 \\ 0 & \tilde{r}(t) \end{pmatrix} \\ &= \begin{pmatrix} 1 & 0 \\ 0 & 1 \end{pmatrix} \quad \Leftrightarrow \quad r(t) = \tilde{r}(t). \end{aligned} \tag{A19}$$

APPENDIX B: TWO REPRESENTATIONS OF A QUANTUM CHANNEL

We will use two different representations. First, we have the "superoperator" representation, which is nothing other than the standard matrix representation of a linear map on a vector space. This representation is easy to read directly from the evolution of a standard set of states; in fact, we shall construct it in that way. Second, there is the Choi-matrix representation in which verifying inherent quantum channel properties is easier.

For the superoperator representation, we represent the density matrices as column vectors, in the so-called "antilexicographical" ordering [40]. For a single qubit, we have

$$\varrho = \begin{pmatrix} \varrho_{00} & \varrho_{01} \\ \varrho_{10} & \varrho_{11} \end{pmatrix} \quad \longleftrightarrow \quad \vec{\varrho} = \begin{pmatrix} \varrho_{00} \\ \varrho_{10} \\ \varrho_{01} \\ \varrho_{11} \end{pmatrix}. \tag{B1}$$

This fixes the matrix representation L_t of the map Λ_t, since the columns of L_t must be the images of the canonical basis vectors. Thus, with the condensed form $\Lambda[ij]_{kl} \equiv \langle k|\,\Lambda_t[\,|i\rangle\langle j|\,]\,|l\rangle$, we obtain

$$L_t = \begin{pmatrix} \Lambda[00]_{00} & \Lambda[10]_{00} & \Lambda[01]_{00} & \Lambda[11]_{00} \\ \Lambda[00]_{10} & \Lambda[10]_{10} & \Lambda[01]_{10} & \Lambda[11]_{10} \\ \Lambda[00]_{01} & \Lambda[10]_{01} & \Lambda[01]_{01} & \Lambda[11]_{01} \\ \Lambda[00]_{11} & \Lambda[10]_{11} & \Lambda[01]_{11} & \Lambda[11]_{11} \end{pmatrix}. \tag{B2}$$

The superoperator representation has the convenient property, that the representation L of the composition of two quantum maps, $\Lambda = \Lambda_2 \circ \Lambda_1$ (where Λ_2 is applied to the result of Λ_1) is simply given by the matrix product of the representations L_1 and L_2 of the individual maps: $L = L_2\, L_1$.

1. Quantum map for intermediate time steps

We know that the superopertor has the following form:

$$L_t = \begin{pmatrix} r & 0 & 0 & 1-r \\ 0 & z_1 & z_2 & 0 \\ 0 & z_2^* & z_1^* & 0 \\ 1-r & 0 & 0 & r \end{pmatrix}, \tag{B3}$$

where r and $z_{1,2}$ are functions on time.

For given quantum maps Λ_t and $\Lambda_{t+\varepsilon}$, we compute the quantum map which takes states $\varrho(t)$ from time t to $t+\varepsilon$. For the moment we assume $\varepsilon > 0$ to be finite. The central question is whether $\Lambda_{t+\varepsilon,t} = \Lambda_{t+\varepsilon} \circ \Lambda_t^{-1}$ is a CP map or not. While the superoperator representation L_t is appropriate to compute the composition of $\Lambda_{t+\varepsilon}$ and Λ_t^{-1}, the Choi representation is needed for verifying the complete positivity. From L_t given on (B3) of Sec. II we have its inverse matrix

$$L_t^{-1} = \begin{pmatrix} r/d & 0 & 0 & (r-1)/d \\ 0 & z_1^*/D & -z_2/D & 0 \\ 0 & -z_2^*/D & z_1/D & 0 \\ (r-1)/d & 0 & 0 & r/d \end{pmatrix}, \tag{B4}$$

where $d = r^2 - (1-r)^2 = 2r-1$ and $D = |z_1|^2 - |z_2|^2$.

If we denote with primes the functions evaluated on $t+\varepsilon$, that is, $r' = r(t+\varepsilon)$ similarly for z_1' and z_2', then

$$L_{t+\varepsilon} = \begin{pmatrix} r' & 0 & 0 & 1-r' \\ 0 & z_1' & -z_2' & 0 \\ 0 & z_2'^* & z_1'^* & 0 \\ 1-r' & 0 & 0 & r' \end{pmatrix}. \tag{B5}$$

We found that the superoperator representation corresponding to $\Lambda_{t+\varepsilon,t}$ is given by

$$L_{t+\varepsilon,t} = L_{t+\varepsilon} L_t^{-1} = \begin{pmatrix} q & 0 & 0 & 1-q \\ 0 & Z_1 & Z_2 & 0 \\ 0 & Z_2^* & Z_1^* & 0 \\ 1-q & 0 & 0 & q \end{pmatrix}, \tag{B6}$$

where $q = (r' - r - 1)/d$, $Z_1 = (z_1' z_1^* - z_2' z_2^*)/D$, and $Z_2 = (z_2' z_1 - z_1' z_2)/D$. The corresponding Choi matrix turns out of reshuffle the above matrix:

$$C_{t+\varepsilon,t} = \begin{pmatrix} q & 0 & 0 & Z_1^* \\ 0 & 1-q & Z_2 & 0 \\ 0 & Z_2^* & 1-q^* & 0 \\ Z_1 & 0 & 0 & q \end{pmatrix}; \tag{B7}$$

in Sec. III A the divisibility of $\Lambda_{t+\varepsilon,t}$ is explored via the positivity (non-negative eigenvalues) of the Choi matrix $C_{t+\varepsilon,t}$.

2. Trace distance and contractivity

We have introduced the trace distance and its definition through of the Eq. (24). Furthermore, it turns out that the trace distance of an Hermitian matrix is equal to one half of the sum of absolute values of its eigenvalues.

Given two any states ϱ_1 and ϱ_2 which evolve under the quantum channel Λ_t, its trace distance at the time t can be calculated as

$$T[\varrho_1(t), \varrho_2(t)] = \tfrac{1}{2}\mathrm{tr}(|\Lambda_t[\varrho_1 - \varrho_2]|); \tag{B8}$$

the right side of the above equation follows from the linearity of Λ_t and due to that $\varrho_i(t) = \Lambda_t[\varrho_i]$. Now, if the states ϱ_1 and ϱ_2 are described by the Bloch vectors $\vec{a} = (a_x, a_y, a_z)$ and $\vec{b} = (b_x, b_y, b_z)$, respectively, we can write

$$T[\varrho_1(t), \varrho_2(t)] = \tfrac{1}{4}\mathrm{tr}(|\Lambda_t[c_x(|0\rangle\langle 1| + |1\rangle\langle 0|) + ic_y(|1\rangle\langle 0| - |0\rangle\langle 1|) + c_z(|0\rangle\langle 0| - |1\rangle\langle 1|)]|), \tag{B9}$$

where the c_is are the vector components of $\vec{c} = \vec{a} - \vec{b}$. Using the linearity of Λ_t and spherical coordinates for $\vec{c} = (R\sin\theta\cos\phi, R\sin\theta\sin\phi, R\cos\theta)$ we have

$$T[\varrho_1(t), \varrho_2(t)] = \frac{1}{4}\mathrm{tr}\left(\left|\begin{pmatrix} R(2r-1)\cos\theta & Re^{-i\,\phi}\sin\theta(z_1^* + e^{i\,2\phi}z_2^*) \\ Re^{i\,\phi}\sin\theta(z_1 + e^{-i\,2\phi}z_2) & -R(2r-1)\cos\theta \end{pmatrix}\right|\right), \tag{B10}$$

which is a Hermitian matrix and therefore

$$T[\varrho_1(t), \varrho_2(t)] = \frac{R\sqrt{(2r-1)^2\cos^2\theta + |z_1 + z_2\, e^{-i\,2\phi}|^2\, \sin^2\theta}}{2}. \tag{B11}$$

[1] L. Landau, Z. Phys. **45**, 430 (1927).
[2] G. Lindblad, Commun. Math. Phys. **48**, 119 (1976).
[3] V. Gorini, A. Kossakowski, and E. C. G. Sudarshan, J. Math. Phys. **17**, 821 (1976).
[4] T. Prosen, New J. Phys. **10**, 043026 (2008).
[5] H. Carmichael, *Statistical Methods in Quantum Optics 1: Master Equations and Fokker-Planck Equations*, Physics and Astronomy Online Library (Springer, New York, 1999).
[6] H.-P. Breuer, E.-M. Laine, and J. Piilo, Phys. Rev. Lett. **103**, 210401 (2009).
[7] Á. Rivas, S. F. Huelga, and M. B. Plenio, Phys. Rev. Lett. **105**, 050403 (2010).
[8] H.-P. Breuer, J. Phys. B: At., Mol. Opt. Phys. **45**, 154001 (2012).
[9] Á. Rivas, S. F. Huelga, and M. B. Plenio, Rep. Prog. Phys. **77**, 094001 (2014).
[10] H.-P. Breuer, E.-M. Laine, J. Piilo, and B. Vacchini, Rev. Mod. Phys. **88**, 021002 (2016).
[11] I. de Vega and D. Alonso, Rev. Mod. Phys. **89**, 015001 (2017).
[12] B.-H. Liu, D.-Y. Cao, Y.-F. Huang, C.-F. Li, G.-C. Guo, E.-M. Laine, H.-P. Breuer, and J. Piilo, Sci. Rep. **3**, 1781 (2013).
[13] D. F. Urrego, J. Flórez, J. Svozilík, M. Nuñez, and A. Valencia, Phys. Rev. A **98**, 053862 (2018).
[14] E. P. Wigner, Ann. Math. **62**, 548 (1955).
[15] T. Guhr, A. Müller-Groeling, and H. A. Weidenmüller, Phys. Rep. **299**, 189 (1998).
[16] P. A. Mello and N. Kumar, *Quantum Transport in Mesoscopic Systems* (Oxford University Press, Oxford, 2004).
[17] T. Prosen and M. Znidaric, J. Phys. A **34**, L681 (2001).
[18] C. Pineda and T. H. Seligman, Phys. Rev. A **75**, 012106 (2007).
[19] C. Pineda, T. Gorin, and T. H. Seligman, New J. Phys. **9**, 106 (2007).
[20] M. Esposito and P. Gaspard, Europhys. Lett. **65**, 742 (2004).
[21] S. A. Gardiner, J. I. Cirac, and P. Zoller, Phys. Rev. Lett. **79**, 4790 (1997).
[22] H. M. Pastawski, P. R. Levstein, G. Usaj, J. Raya, and J. Hirschinger, Physica A (Amsterdam) **283**, 166 (2000).
[23] F. Haug, M. Bienert, W. P. Schleich, T. H. Seligman, and M. G. Raizen, Phys. Rev. A **71**, 043803 (2005).
[24] M. V. S. Bonança and M. A. M. de Aguiar, Phys. Rev. A **74**, 012105 (2006).
[25] C. Pineda, T. Gorin, D. Davalos, D. A. Wisniacki, and I. García-Mata, Phys. Rev. A **93**, 022117 (2016).
[26] J. L. Lebowitz and L. Pastur, J. Phys. A: Math. Gen. **37**, 1517 (2004).
[27] M. Carrera, T. Gorin, and T. H. Seligman, Phys. Rev. A **90**, 022107 (2014).
[28] M. L. Mehta, *Random Matrices and the Statistical Theory of Energy Levels,* 3rd ed. (Academic Press, New York, 2004).
[29] T. Gorin, T. Prosen, T. H. Seligman, and W. T. Strunz, Phys. Rev. A **70**, 042105 (2004).
[30] M.-D. Choi, Linear Algebra Appl. **10**, 285 (1975).
[31] M. Ziman and T. Heinosaari, *The Mathematical Language of Quantum Theory* (Cambridge University Press, Cambridge, 2012).
[32] N. G. van Kampen, *Stochastic Processes in Physics and Chemistry* (North-Holland, Elsevier, 2007).
[33] M. A. Nielsen and I. L. Chuang, *Quantum Computation and Quantum Information* (Cambridge University Press, Cambridge, 2000).
[34] S. Wißmann, A. Karlsson, E.-M. Laine, J. Piilo, and H.-P. Breuer, Phys. Rev. A **86**, 062108 (2012).
[35] D. Chruściński, A. Kossakowski, and A. Rivas, Phys. Rev. A **83**, 052128 (2011).
[36] G. M. Cabrera, D. Davalos, and T. Gorin, Phys. Lett. A **383**, 2719 (2019).

[37] H.-P. Breuer and F. Petruccione, *The Theory of Open Quantum Systems* (Oxford University Press, Oxford, 2002).

[38] E. Merzbacher, *Quantum Mechanics* (Wiley, New York, 1998).

[39] L. Roa, A. Muñoz, and G. Grüning, Phys. Rev. A **89**, 064301 (2014).

[40] I. Bengtsson and K. Zyczkowski, *Geometry of Quantum States: An Introduction to Quantum Entanglement* (Cambridge University Press, Cambridge, 2006).